

Article

Development of Intensity–Duration–Frequency (IDF) Curves over the United Arab Emirates (UAE) Using CHIRPS Satellite-Based Precipitation Products

Tareefa S. Alsumaiti ¹, Khalid A. Hussein ^{1,2,*} , Dawit T. Ghebreyesus ³ , Pakorn Petchprayoon ⁴, Hatim O. Sharif ⁵  and Waleed Abdalati ²

¹ Geography and Urban Sustainability Department, College of Humanities and Social Sciences, United Arab Emirates University, Al Ain P.O. Box 15551, United Arab Emirates; tareefa@uaeu.ac.ae

² Cooperative Institute for Research in Environmental Sciences (CIRES), University of Colorado, Boulder, CO 80309, USA; waleed.abdalati@colorado.edu

³ Bridgefarmer & Associates, Inc., 2350 Valley View Lane, Suite 600, Dallas, TX 75234, USA; dawittesfaldet@gmail.com

⁴ Geo-Informatics and Space Technology Development Agency (GISTDA), Bangkok 10210, Thailand; pakorn@gistda.or.th

⁵ Department of Civil and Environmental Engineering, University of Texas at San Antonio, San Antonio, TX 78249, USA; hatim.sharif@utsa.edu

* Correspondence: khalid.hussein@uaeu.ac.ae

Abstract: The recent flooding events in the UAE have emphasized the need for a reassessment of flood frequencies to mitigate risks. The exponential urbanization and climatic changes in the UAE require a reform for developing and updating intensity–duration–frequency (IDF) curves. This study introduces a methodology to develop and update IDF curves for the UAE at a high spatial resolution using CHIRPS (Climate Hazards Group InfraRed Precipitation with Station) data. A bias correction was applied to the CHIRPS data, resulting in an improved capture of extreme events across the country. The Gumbel distribution was the most suitable theoretical distribution for the UAE, exhibiting a strong fit to the observed data. The study also revealed that the CHIRPS-derived IDF curves matched the shape of IDF curves generated using rain gauges. Due to orographic rainfall in the northeastern region, the IDF intensities were at their highest there, while the aridity of inland regions resulted in the lowest intensities. These findings enhance our understanding of rainfall patterns in the UAE and support effective water resource management and infrastructure planning. This study demonstrates the potential of the CHIRPS dataset for IDF curve development, emphasizes the importance of performing bias corrections, and recommends tailoring adjustments to the intended application.

Keywords: remote sensing; CHIRPS; precipitation; UAE; water resources



Citation: Alsumaiti, T.S.; Hussein, K.A.; Ghebreyesus, D.T.; Petchprayoon, P.; Sharif, H.O.; Abdalati, W. Development of Intensity–Duration–Frequency (IDF) Curves over the United Arab Emirates (UAE) Using CHIRPS Satellite-Based Precipitation Products. *Remote Sens.* **2024**, *16*, 27. <https://doi.org/10.3390/rs16010027>

Academic Editors: Steven Dewit and Yuriy Kuleshov

Received: 10 July 2023

Revised: 28 November 2023

Accepted: 18 December 2023

Published: 20 December 2023



Copyright: © 2023 by the authors. Licensee MDPI, Basel, Switzerland. This article is an open access article distributed under the terms and conditions of the Creative Commons Attribution (CC BY) license (<https://creativecommons.org/licenses/by/4.0/>).

1. Introduction

Precipitation is one of the main and most significant components of the water cycle that drives water from the atmosphere to the lithosphere and biosphere. These interactions have a substantial influence on the climate dynamics of ecosystems [1]. The long- and short-term variability in precipitation has a very vital impact on the environment; this is particularly true for countries located in arid regions, such as the United Arab Emirates (UAE) [2,3]. Thus, capturing the variability in precipitation is crucial to forecasting the climate. The main hurdle in estimating the variability in precipitation is its highly intermittent nature in both temporal and spatial domains.

The scientific community has been developing various techniques for capturing the temporospatial variability in precipitation using conventional and unconventional methods [4]. The advancement of satellites and sensors over the last four decades has led to the

near-real-time derivation of high-resolution global precipitation products and the development of sophisticated remote-sensing techniques [5]. These, combined with the exponential improvement in computational power, make it possible to capture precipitation variability.

Remotely sensed precipitation products have been used in a wide range of scientific fields, such as meteorology, hydrometeorology, climatology, and water resources management [6]. Satellite-based products, in particular, offer significant advantages in simulating hydrological processes within vast, ungauged watersheds, especially in regional river basins where acquiring and utilizing precipitation observations pose challenges [7]. Numerous studies evaluating and validating remotely sensed products worldwide have concluded that these products exhibit a high potential for capturing the spatial and temporal distribution of precipitation across diverse topographic features [8–12]. The main strength of remotely sensed precipitation products is the ability to capture the spatial distribution of rainfall. Furthermore, studies have revealed that these products improve as they evolve over time [11,13,14]. They also provide accessibility to remote areas, which is a massive advantage over conventional methods. However, products that incorporate ground-based measurements are more robust and accurate relative to those that only use remotely sensed data [11,15,16]. One prevalent drawback of products is their lack of consistency across different regions worldwide and varying climatic conditions. Geographic characteristics, such as elevation, longitude, and latitude, are the primary factors contributing to this inconsistency [17]. Therefore, localized adjustments are recommended prior to their application.

Climate Hazards Group InfraRed Precipitation with Station (CHIRPS) data are a quasi-global rainfall estimate from in situ and satellite observations. CHIRPS was developed by the United States Geological Survey (USGS) and Climate Hazards Center (CHC) scientists with the main goal of being used for long-term hydrological studies and environmental monitoring over remote areas with sparse ground-based observations. Over the years, numerous validation studies have been conducted across the globe. Rivera and Marianetti [18] evaluated the product for an extended period (30 years) over the Central Andes of Argentina. Their results showed a good correlation with 57 rain gauge records. However, their analysis also revealed systematic overestimation errors attributed to high-altitude areas. Another study [19] conducted in Turkey found that CHIRPS has a high probability of detection (more than 0.86) with a false alarm rate of 0.13 for a threshold of 5 mm/month. The product performed better in flat regions than in mountainous areas. Additionally, the product's performance was significantly influenced by the type of rainfall regime and it was better at capturing cyclonic precipitation. The authors concluded that CHIRPS is well suited for hydro-climatological studies.

Wang and Petersen [15] evaluated the accuracy of CHIRPS precipitation estimates over mainland China. The authors found that CHIRPS was generally accurate, but it underestimated the precipitation in some mountainous regions. Hsu and Huang [20] evaluated the performance of CHIRPS in depicting the precipitation variation over multiple timescales in Taiwan. The authors stated that CHIRPS was better than the Integrated Multi-satellite Retrievals for Global Precipitation Mission (IMERG) in representing the magnitude of the annual cycle of monthly precipitation, the spatial distribution of the seasonal mean precipitation for all four seasons, and the quantitative precipitation estimation of the interannual variation in area-averaged winter precipitation in Taiwan. CHIRPS was also assessed for modeling hydrological processes. Luo and Wu [7] found that the product was superior to rain gauges and the inverse distance weighted (IDW) interpolation of the data for forcing the Soil and Water Assessment Tool (SWAT) model of the Lower Lancang-Mekong River Basin. Another study conducted across India reinforced the suitability of CHIRPS for long-term analysis applications with a high level of confidence [21]. The study compared four multi-satellite precipitation products against rain gauges and found that CHIRPS and TRMM were the best products across India. The main advantage of CHIRPS over other satellite-based products is the over 40-year length of the record, which is long enough to conduct climatological studies. Most other remote sensing products have a

historic record of less than two decades, which may not provide enough data to accurately estimate the parameters for the IDF curve, as such curves typically require long-term rainfall data to develop reliable estimates [22].

An intensity–duration–frequency (IDF) curve is a statistical tool that estimates the probability of extreme precipitation events. It is derived from long-term historical observations and serves as a crucial input for engineering design purposes [23]. In light of the dynamic and evolving nature of the climate, particularly with respect to extreme events, frequent updates to IDF curves are essential to ensure their accuracy and relevance [22]. Studies have consistently demonstrated an upward trend in the frequency and magnitude of extreme precipitation events across various regions of the world [24–26]. Conventional IDF curves rely on ground-based precipitation measurements. However, the sparse and uneven distribution of these measurements often fails to capture the true spatial variability in rainfall, leading to potential biases in the derived IDF curves [27]. Despite the robust statistical framework underlying IDF development, inherent biases introduced by interpolation and other spatial distribution techniques can introduce significant uncertainties [28]. These challenges are particularly prevalent in developing countries where historical data are limited to a few decades and rain gauge networks are heavily concentrated in urban areas, leaving rural areas underserved. Furthermore, the task of constructing IDF curves from a network of rain gauges with diverse historical records, maintained by different entities without standardized quality control and calibration procedures, employing heterogeneous measuring techniques, and exhibiting varying degrees of precision, poses a considerable challenge [29].

In the last two decades, many scientists and researchers across the globe have assessed the potential of these remotely sensed precipitation products for developing IDF curves. CMORPH was used over the Eastern Mediterranean [30]; Global Satellite Mapping of Precipitation (GSMaP) was applied in Singapore [31]; GPM products were evaluated over the Alpine forelands of Austria and in a semi-arid region of the United States (Alcely Lua); a radar network of the USA was evaluated over the state of Texas [22]; and PERSIANN—Climate Data Record (PERSIANN-CDR) was evaluated over the contiguous United States (CONUS) [28], to name a few of the studies. All these studies showed a high correlation between the developed IDF curves and the IDFs developed using conventional methods. The potential of using remotely sensed products in hydrometeorological studies was shown across different terrains and over a wide range of latitudes. However, these products lack the long-spanning historical data, except for CHIRPS, needed to capture climatological cycles, which are essential for developing IDF curves.

The aim of the present study is to develop spatially distributed IDF curves over the UAE by employing a historically rich dataset from CHIRPS. The main objective is to produce IDF curves that will fill the gaps created by the sparsely distributed rain gauges. Furthermore, this study will advance our knowledge of the application of CHIRPS data in developing IDF curves, especially for extreme event analyses. This research also evaluates the viability of CHIRPS data in an arid region with a very dry climate. The manuscript is organized as follows: Section 2 describes the study area and the dataset used in the study. The methodology, which includes all the necessary equations and assumptions, is presented in Section 3. The results of the study are discussed in Section 4. Finally, the summary and recommendations of the study are provided in Section 5.

2. Study Area and Dataset

2.1. Study Area

The UAE is situated between the UTM coordinates of 2,883,648 m Northing 40R and 2,503,242 m Northing 40Q and 559,185 Easting 39R and 437,054 Easting 40R in the southeast of the Arabian Peninsula (Figure 1). The UAE covers an area of around 83,600 km², with geomorphologic features ranging from mountainous regions in the northeastern part to sand dunes covering the majority of the western parts of the country [32]. The Al Hajar Mountain Range, located near the border with Oman, forms the highest topography of the

UAE, reaching a peak altitude of 1800 m, causing the area to be the wettest and coolest part of the country [33]. The nation has a long stretch of coastline, which controls the climate dynamics of the country. It borders the Arabian Gulf in the north and the Gulf of Oman in the east. The country's precipitation regime is influenced by these major water bodies, as major sources of moisture. According to the Köppen climatic classification, the entire nation has an arid, hot desert climate (BWh). As per the National Center of Meteorology (NCM), the monthly average temperature reaches its peak in August at 40.3 °C. Mountainous areas typically have colder winter temperatures that drop to near freezing. Humidity levels can reach as high as 95% at the end of summer due to strong southeasterly breezes. The entire area experiences dry weather all year. Low rainfall infiltration into wadi beds and flash flooding are common in places that are downstream of mountainous regions. Water from the high altitude, with its huge amount of energy, can cause dangerous flash floods in a very short period of time.

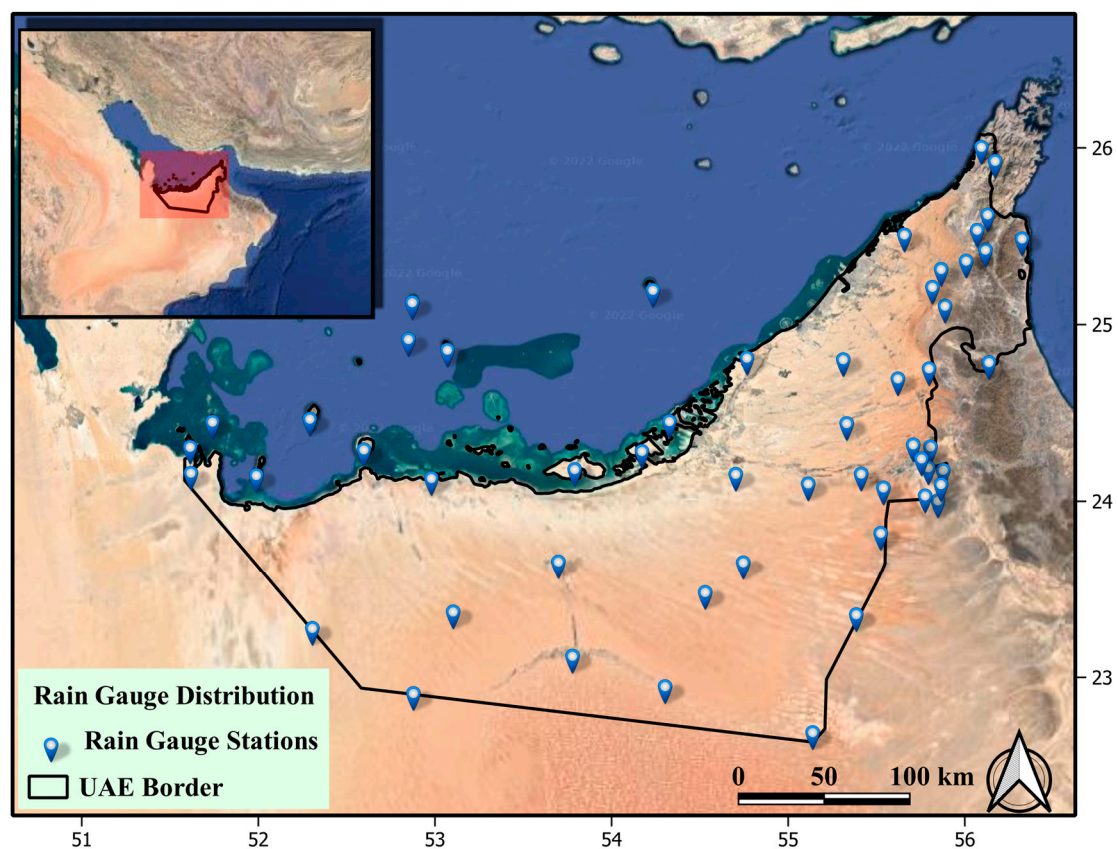


Figure 1. Map showing the study area and the distribution of the rain gauge stations across the United Arab Emirates (UAE). The x and y axes represent the longitude (east) and latitude (north) in degrees, respectively.

2.2. Datasets

2.2.1. Rain Gauge Data

The main goal of this study is to explore the potential of the CHIRPS dataset for developing IDF curves. However, rain gauges were used to locally calibrate the systematic bias of CHIRPS in the area. Data from a network of 54 rain gauges distributed across the country were obtained from the NCM of the UAE. The time frame of the coverage of the rain gauges is from 2003 to 2021, except for Abu Dhabi Airport, which covers 1983 to 2021. The network of the rain gauges is managed and quality-controlled by the NCM. The rain gauges have a temporal resolution of 15 min. The spatial distribution of the rain gauges is shown in Figure 1. The network is new, with most rain gauges having a temporal coverage of less than 20 years in addition to their sporadic distribution. Moreover, the distribution of

the rain gauges is uneven, with most of them concentrated in urban centers. The spatial distribution of the annual average rainfall shows that the wettest regions are located in the northeastern part of the country, where the Al Hajar Mountains are located (Figure 2A).

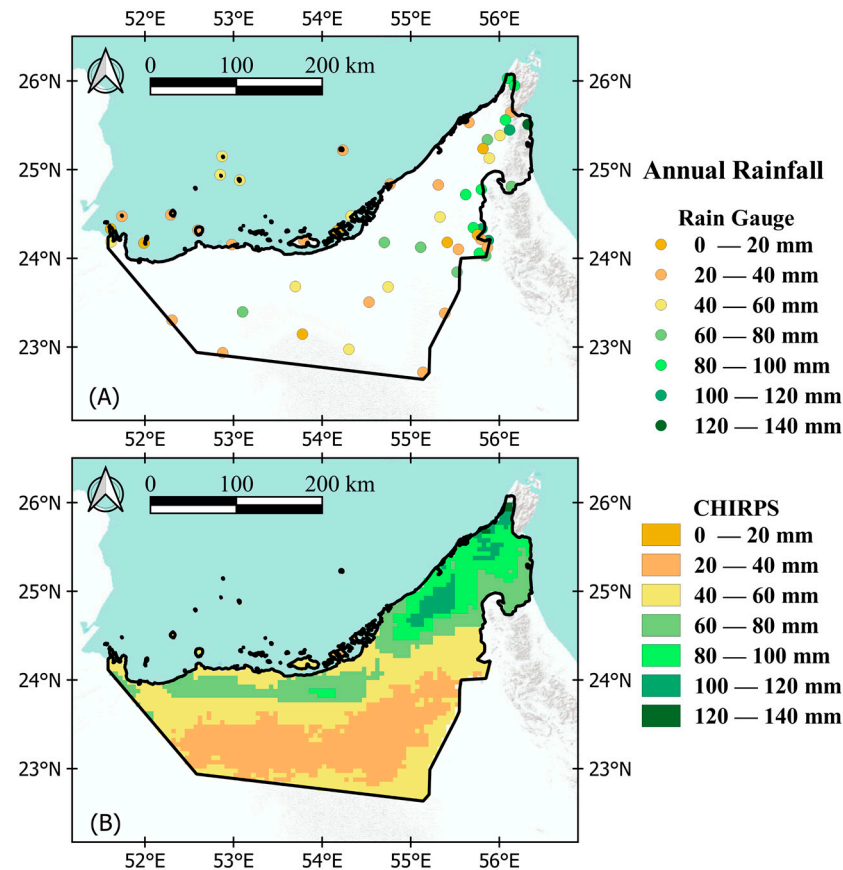


Figure 2. Spatial distribution of the average annual rainfall of the UAE (A) observed from the in situ rain gauge stations and (B) estimated by CHIRPS.

2.2.2. CHIRPS Precipitation Product

CHIRPS was developed by a partnership of scientists from the USGS Earth Resources Observation and Science (EROS) Center and the Climate Hazard Center (CHC) at the University of California, Santa Barbara, to provide a complete, reliable, and up-to-date dataset for a variety of early warning objectives, such as trend analyses and drought monitoring. The dataset has a quasi-global spatial terrestrial coverage (50°S–50°N) with a high spatial resolution (0.05°) and daily temporal resolution. The CHIRPS dataset was produced by integrating precipitation estimates based on infrared cold cloud duration (CCD) observations that were calibrated using the TRMM Multi-Satellite Precipitation Analysis (MSPA) and in situ station data [34–36]. The anchor stations that were used for calibrating this product are from regional and national meteorological services that are available in the public domain. The CHIRPS dataset was downloaded from the website (<https://www.chc.ucsb.edu/data/chirps>, accessed on 1 August 2023) for the years 1981–2021. The high spatial resolution of the CHIRPS dataset, combined with its long historical record compared to that of other remotely sensed products, makes it a suitable candidate for analyzing and simulating hydrological processes even in relatively small and localized catchments.

The spatial distribution of the annual average rainfall of the UAE was captured with reasonable accuracy by CHIRPS, as shown in Figure 2B. Similar to the rain gauges, the wettest regions were found to be in the northeastern parts of the country. The coastal areas showed higher levels of precipitation relative to the records from the rain gauges. This is a

common issue with remotely sensed products, as they misinterpret the moisture near the ground surface as rainfall, especially in humid areas like the UAE's coastal areas [11,37–39].

3. Methodology

3.1. Bias Correction

As mentioned earlier, most satellite-based precipitation products require localized adjustments to address potential biases before their application. This step is particularly crucial when utilizing these products to evaluate extreme events such as IDF and droughts, as they often exhibit underestimations or overestimations of such events [11,17,40]. To address these biases, linear modeling was employed in conjunction with rain gauge observations. Given the focus on IDF, the analysis solely considered extreme rainfall events; rainfall exceeding the 95th percentile of the annual precipitation distribution was filtered for bias correction. This approach minimizes the potential bias introduced by the strong correlation between the daily average rainfall and the correction factor [28]. First, daily rainfall events exceeding the 95th percentile were extracted from each year's rain gauge records. Subsequently, the corresponding rainfall estimates for those days derived from CHIRPS were matched. The adjustment factor (ζ) is defined by the ratio of ground-based observations to satellite-based precipitation (CHIRPS) and was calculated for the entire study area. A calibration and validation analysis were conducted to measure and correct the bias and to evaluate the performance of the bias adjustment. The calibration phase was carried out for the first nine years of the data, from 2003 to 2011, and a validation was performed for the rest of the time frame, i.e., from 2012 to 2021.

$$\zeta = \frac{R_G}{R_S} \quad (1)$$

where ζ is the correction factor of each rain gauge, R_G is the rainfall in situ record, and R_S is the estimate of CHIRPS precipitation corresponding to that record.

3.2. Performance Criteria

The evaluation of the bias correction factor was conducted using statistical performance metrics: the Pearson's correlation coefficient (CC), percentage bias (RBIAS), root mean squared error (RMSE), Nash–Sutcliffe efficiency (NSE), and Kling–Gupta efficiency (KGE). The Kling–Gupta model efficiency coefficient metric estimates the goodness-of-fit of a model. This coefficient has three main components: correlation, bias, and variability. The equations of all the metrics used in this study with their respective perfect values are presented in Table 1. These metrics are widely used to assess the performance of models in hydrological studies, especially those related to precipitation [11,41].

Table 1. List of the statistical performance metrics used for the evaluation of the correction factor.

Statistical Index	Units	Equation	Perfect Value
Pearson's correlation coefficient (CC)	Ratio	$CC = \frac{\sum_{i=1}^n (G_i - \bar{G})(S_i - \bar{S})}{\sqrt{\sum_{i=1}^n (G_i - \bar{G})^2} \sqrt{\sum_{i=1}^n (S_i - \bar{S})^2}}$	1
Percentage Bias (RBIAS)	%	$PBIAS = \frac{\sum_{i=1}^n (S_i - G_i)}{\sum_{i=1}^n G_i} * 100$	0
Root Mean Squared Error (RMSE)	mm	$RMSE = \sqrt{\frac{1}{n} * \sum_{i=1}^n (S_i - G_i)^2}$	0
Nash–Sutcliffe Efficiency (NSE)	Ratio	$NSE = 1 - \frac{\sum_{i=1}^n (G_i - S_i)^2}{\sum_{i=1}^n (G_i - \bar{G})^2}$	1
Kling–Gupta Efficiency (KGE)	Ratio	$NSE = 1 - \sqrt{(r-1)^2 + \left(\frac{\sigma_S}{\sigma_G} - 1\right)^2 + \left(\frac{\bar{S}}{\bar{G}} - 1\right)^2}$	1

where G_i is the gauge observation; S_i is the satellite estimation; \bar{G} is the mean of the gauge observation; \bar{S} is the mean of the satellite estimation; n is the number of observations; r is the linear correlation coefficient; σ_S is the standard deviation of the satellite estimates; and σ_G is the standard deviation of the gauge observations.

3.3. IDF Development

The main objective of this study is to assess the performance of CHIRPS in developing IDF curves over an arid region with very limited ground-based observations and provide an efficient alternative method. IDF is a graphical representation of the rainfall intensity with its duration and annual frequency, which is developed using a theoretical distribution that has a robust statistical background. The development of IDF curves involves finding the best statistical distribution that explains the variability in the extreme precipitation values for a given location. The first step is to apply the spatially distributed correction factor to the CHIRPS dataset. The next step is to extract the annual maxima series (AMS) of the rainfall event over a long period of time, which is enough to fit a theoretical extreme distribution model. In this study, the AMS for six rainfall events (1-day to 6-day) for 41 years (1981–2021) was used to fit a statistical distribution model. The spatially distributed IDF analysis was conducted across the entire country to generate IDF curves for ungauged rural areas. Additionally, IDF curves were developed for eight major cities in the UAE, offering an alternative to the conventional point-based analysis. These cities include Al Ain, Abu Dhabi, Ajman, Dubai, Fujairah, Ras Al Khaimah, Sharjah, and Umm Al Quwain.

This study assessed the suitability of commonly used theoretical distributions, recommended by Ghebreyesus and Sharif [22], for analyzing extreme events in arid and semi-arid regions. The aim was to identify the distribution that exhibits the best fit and adheres to stringent “goodness-of-fit” criteria. We employed the GEV and Gumbel distributions from the generalized extreme value (GEV) distribution family, and from the generalized Pareto (GP) distribution family, the GP and exponential distributions were implemented. Most extreme value distributions have three parameters that represent the location, scale, and shape of the distribution. Gumbel is a special case of distribution in the GEV family in which the shape parameter is zero, and the exponential distribution is a unique case of the GP distribution family in which both the shape and scale parameters are assumed to be zero. The estimation of the parameters was performed using the generalized maximum likelihood estimation (GMLE) method, which has proven to be the best method for data with small sample sizes, as in the case of developing IDFs [42,43]. The goodness of fit of the four theoretical distributions was evaluated using the Kolmogorov–Smirnov test [44]. This widely used non-parametric test is popular across diverse disciplines due to its independence from the underlying distribution. Moreover, the test is robust and has less sensitivity to outliers at each tail of the distribution. The methodology followed for this study is summarized in Figure 3. The IDF curves were developed for common return periods, which represent the probability of the recurrence of storm events.

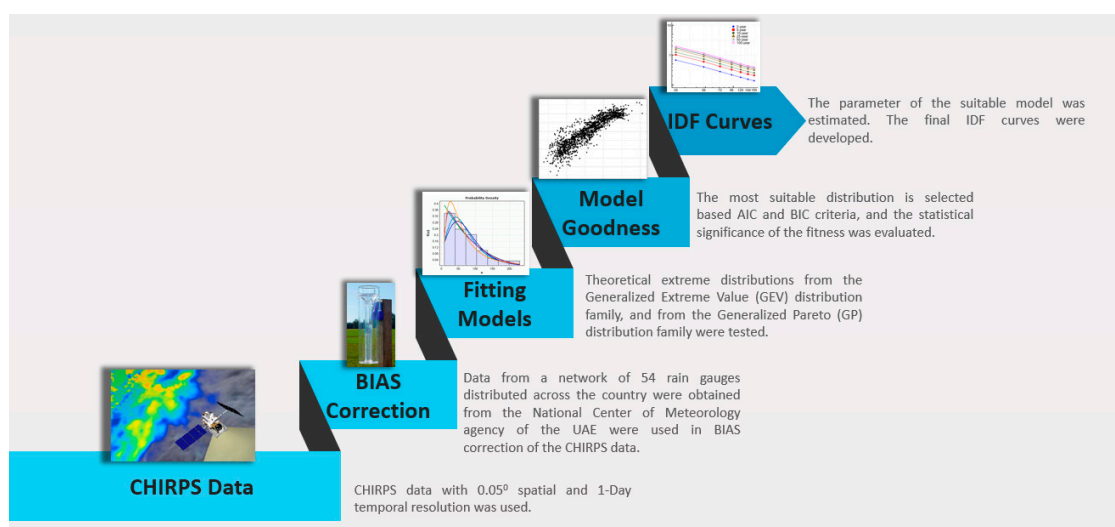


Figure 3. Flow chart of the study methodology.

4. Results and Discussion

4.1. Bias Correction

The CHIRPS data bias was adjusted using observational data from 54 rain gauge stations in order to improve its accuracy. The bias correction factor was determined by comparing the CHIRPS estimates with the rain gauge observations. The effectiveness of the correction factor is summarized in Table 2, which provides the details of its performance. During the calibration phase, the bias correction factor displayed a remarkably high correlation coefficient of 0.84. In the subsequent validation phase, the correlation coefficient was still significant at 0.63. This indicates that the correction factor performed well in terms of aligning the CHIRPS data with the observed values. The evaluation metrics presented in the table, such as the KGE, NSE, and bias percentage, further support the excellent performance of the correction factor. The presence of bias suggests that the CHIRPS product tends to underestimate high-intensity precipitation over the UAE. This finding aligns with previous studies that have assessed satellite-based precipitation products in the region. It is worth noting that satellite-based precipitation products often struggle to accurately capture heavy storms while tending to overestimate lighter storms, particularly in arid and semi-arid regions (e.g., Alsumaiti, Hussein [11]; Ghebreyesus and Sharif [22]).

Table 2. Summary of the performance metrics for the calibration and validation phases.

Performance Metric	Calibration	Validation
Pearson Correlation Coefficient	0.84	0.63
Kling–Gupta Efficiency (KGE)	0.81	0.53
Nash–Sutcliffe Efficiency (NSE)	0.82	0.43
Percent Bias (%)	5.10	−13.20
Root Mean Square Error (mm)	1.68	10.80

Figure 4 presents the scatter plots of the rain gauge versus the satellite product (CHIRPS) for both the calibrated and validated data. The scatter plots show that the bias correction improved the CHIRPS product as the correlation increased.

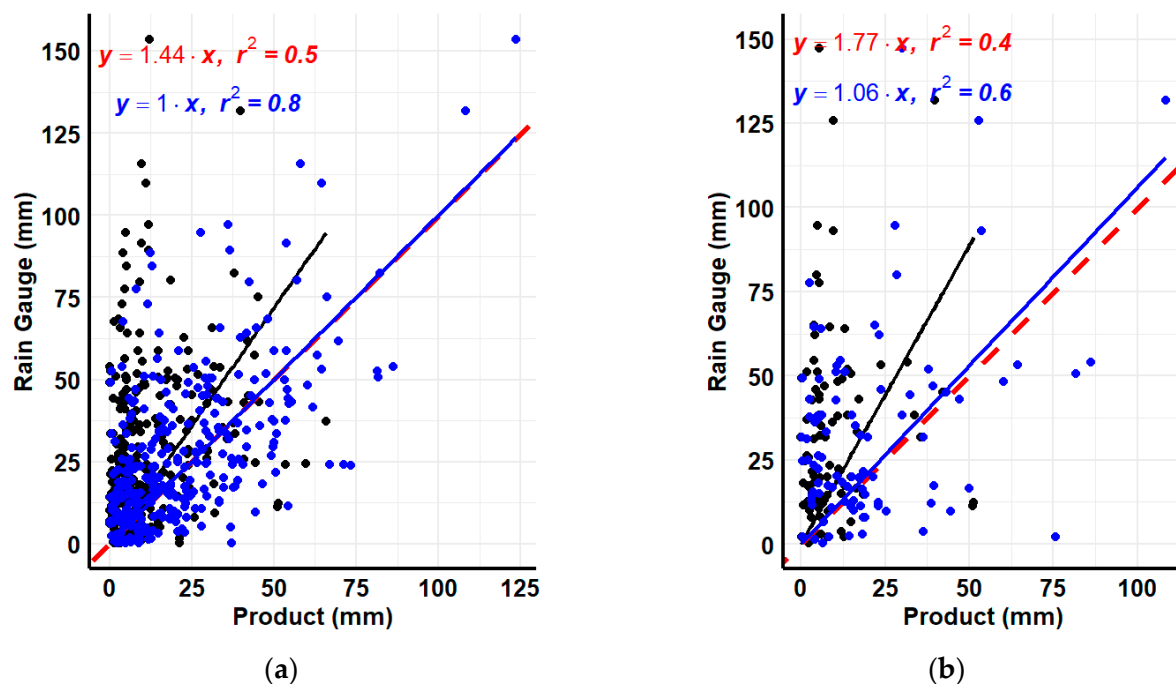


Figure 4. Scatter plot of rain gauge versus CHIRPS for (a) calibration phase and (b) validation phase (black represents raw data; the red equation is between CHIRPS raw data and rain gauge; blue represents bias-corrected data; and the red dotted line shows $y = x$).

Overall, the CHIRPS product underestimated the extreme events across the country, as shown in the spatial distribution of the bias correction. The average bias factor across the country was 3.25, ranging from as low as 1.5 in the northeastern part of the country to as high as 5.25 in the southern part of the country, as shown in Figure 5. However, the southern and western parts of the country showed the highest underestimation. This is because these regions are the driest parts of the country. The product performed better in capturing the extreme events in the northeastern part of the country, where the annual average rainfall is the highest. The CHIRPS dataset has been documented to have limitations in capturing extreme events in arid and semi-arid areas, which are considered one of its main weaknesses [45]. The reason for this could be the high intensity and short duration of the rainfall in arid and semi-arid regions. This behavior is not unique to CHIRPS; most satellite-based precipitation products have the same problem [11,46].

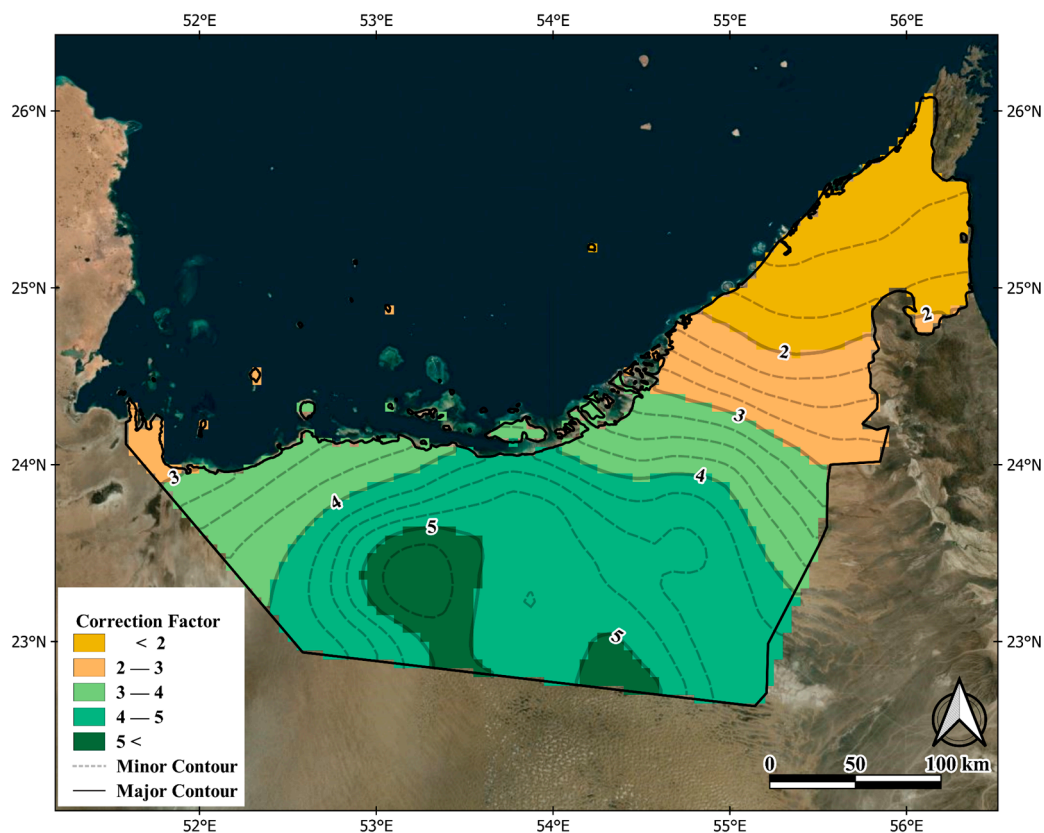


Figure 5. Spatial distribution of the bias correction factor.

4.2. Development of IDF Curves

The process of the IDF's development involved a systematic approach, as outlined in Section 3. The results of the analysis, illustrated below, signify the successful implementation of the IDF curve development process. The study findings provide valuable insights into extreme rainfall characteristics, distribution models, and spatial patterns within the UAE.

4.2.1. Fitting Statistical Distributions

The different storm event durations were fitted to four theoretical extreme value distributions. The best distribution that represents the distribution of the AMS was selected using performance criteria. The most widely used performance criteria to assess the goodness of distribution are the Bayesian information criterion (BIC) and the Akaike information criterion (AIC). The best distribution that fits the AMS was found to be the Gumbel distribution in the majority of the country over all the storm duration events.

Interestingly, as the duration of the storm event increases, the Gumbel distribution becomes the best distribution across the country (Figure 6). For the 1-day storm event, Gumbel was found to have the best distribution in 52% of the country. This steadily increased to 74% as the storm event duration increased to a 4-day event, then decreased.

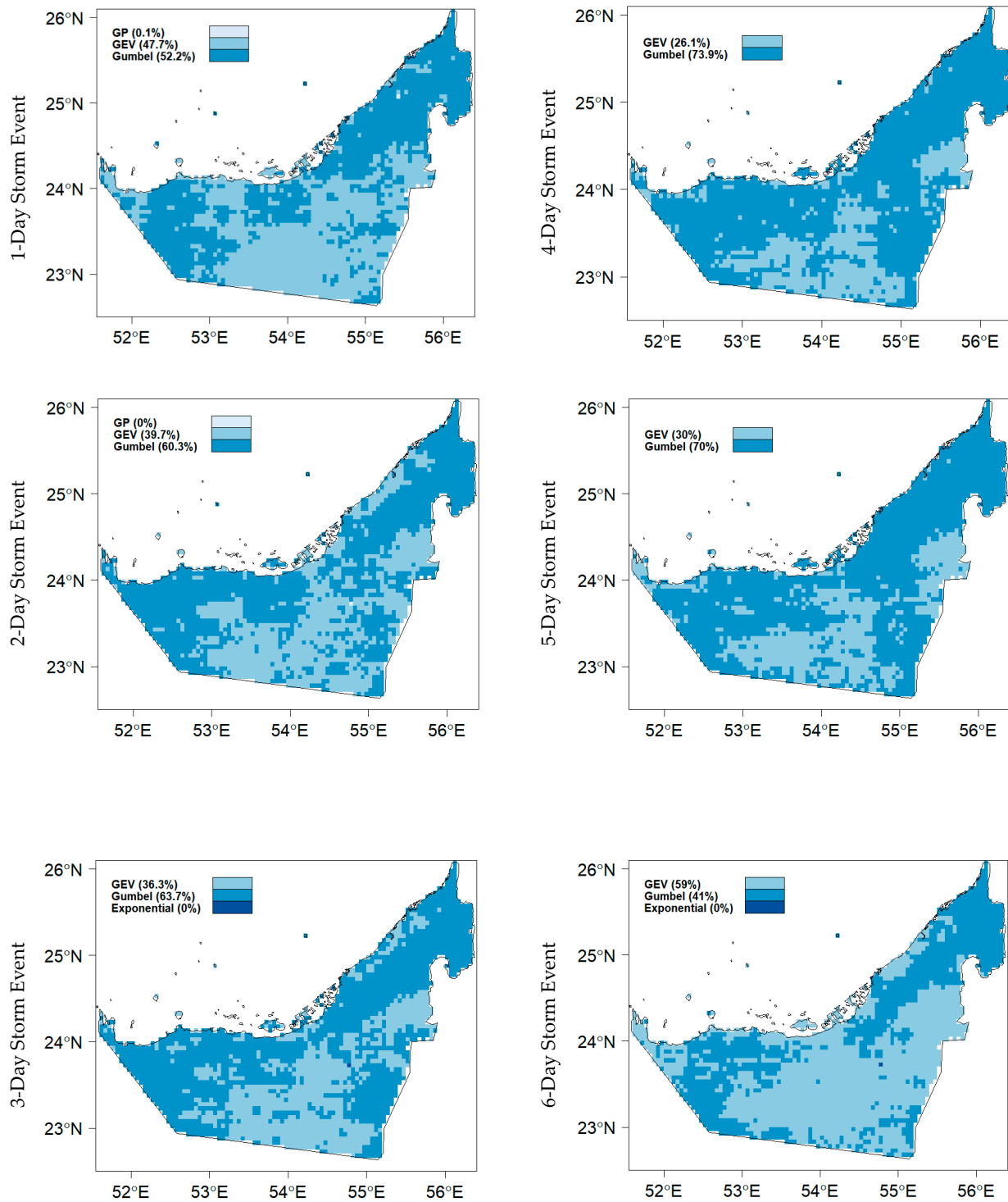


Figure 6. The spatial distribution of the suitable theoretical extreme distributions (generalized extreme, GEV; Gumbel; generalized Pareto, GP; exponential) for different storm event durations (1-day to 6-day) across the country (UAE).

The Gumbel distribution demonstrated suitability across coastal areas and the north-eastern region of the country. In contrast, the annual maximum series (AMS) of the southern regions exhibited a stronger correlation with the GEV distribution. Overall, the GP and exponential distributions displayed the weakest correlations across the entire country for all storm event durations. These findings align with previous studies conducted in the country (Sherif, Chowdhury [47]; Almheiri, Rustum [48]). The GEV distribution family proved to be a more suitable model for AMS in arid and semi-arid regions compared to the GP distribution family.

Violin plots were utilized to visualize the distributions of the AIC and BIC across all durations, as depicted in Figure 7. It is important to note that when employing the AIC and BIC for model selection, the parameter value itself does not hold significant meaning; however, the model with the lowest values indicates the best fit. In Figure 7, it is evident that the GEV and Gumbel distributions exhibit the lowest mean and median values for both the AIC and BIC. Upon comparing the means and medians of these distributions, the Gumbel distribution consistently demonstrates the lowest AIC and BIC values across all storm durations. On the other hand, the exponential distribution represents the weakest fit. The observed increase in the AIC and BIC values with longer storm durations can be attributed to the higher volume of precipitation during those periods.

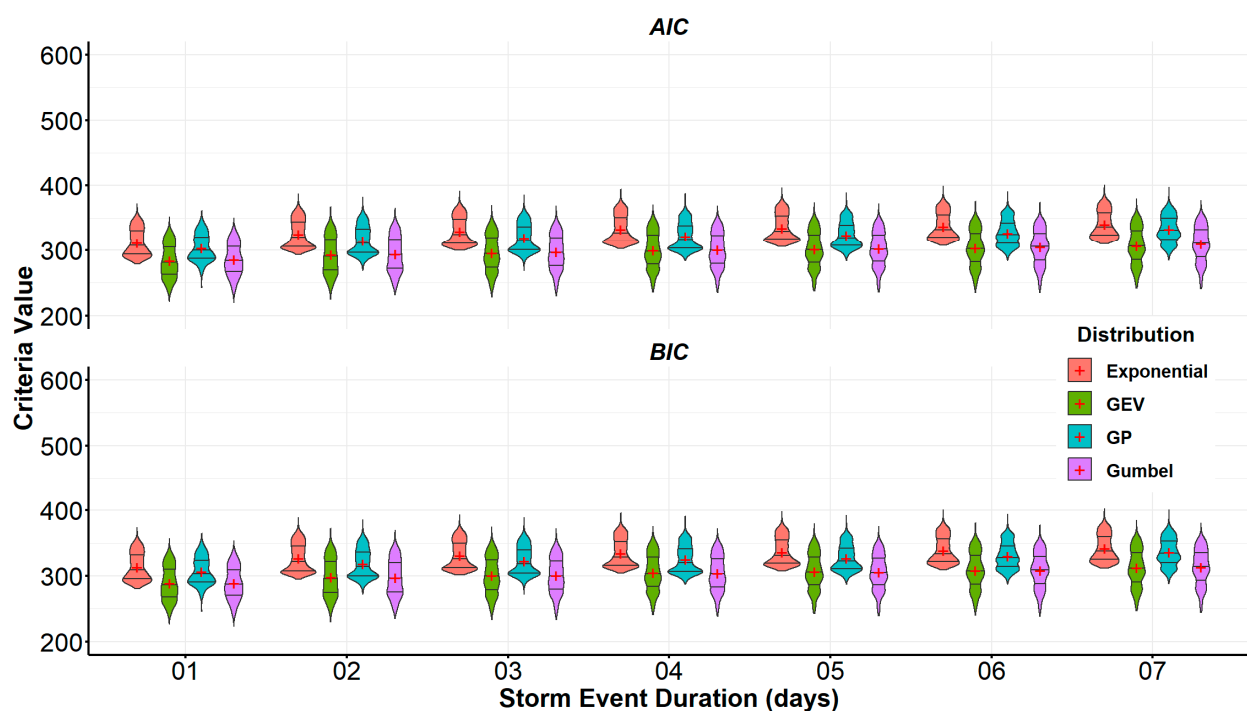


Figure 7. The violin diagram showing the results of the performance criteria (Bayesian information criterion and Akaike information criterion) used to evaluate the goodness of fit of the four theoretical distributions (GEV, Gumbel, GP, and exponential) tested across the country (UAE).

Given its dominance and superior goodness of fit across most of the country for all storm event durations, the Gumbel distribution was selected as the primary model for developing IDF curves. The statistical significance of the Gumbel distribution was rigorously evaluated using the Kolmogorov–Smirnov test. The results revealed that the Gumbel distribution adequately fit the event distribution in over 96% of the country for all storm event durations. To further assess the statistical significance across different locations, the spatial distribution was examined, as depicted in Figure 8. It was observed that areas lacking statistical significance were primarily concentrated in the western region of the country. This observation aligns with expectations, as the western part is known to be the driest area within the country.

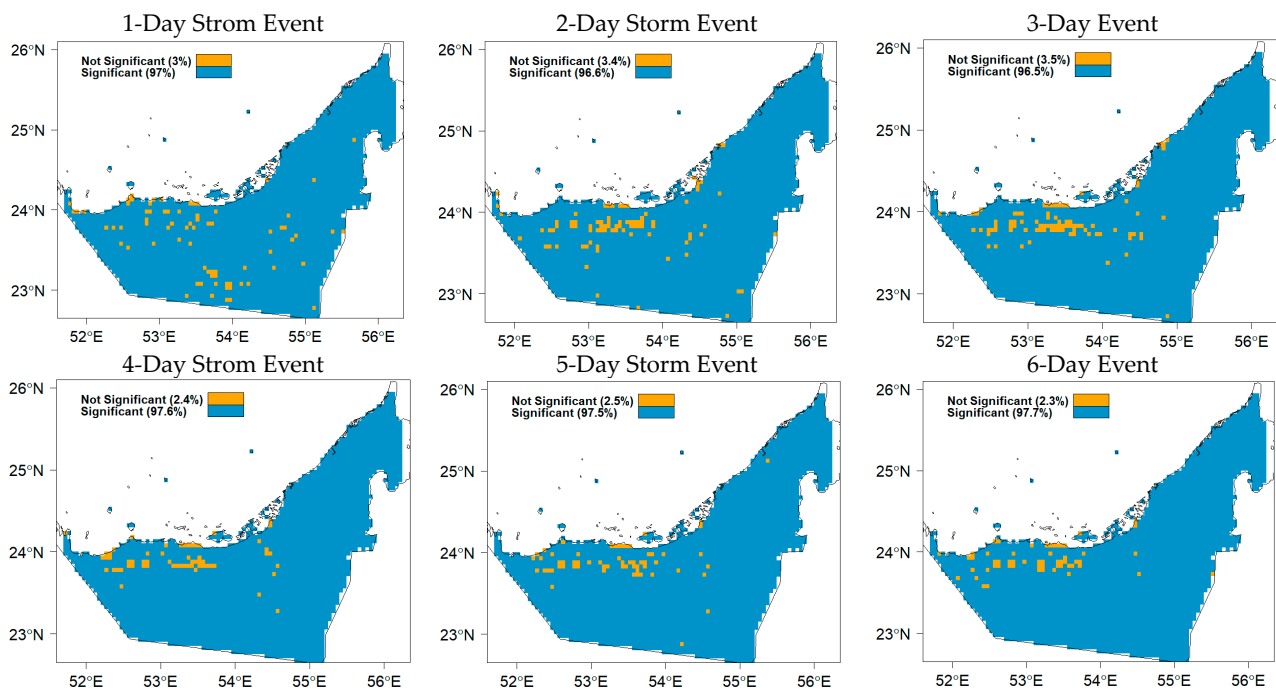


Figure 8. The spatial distribution of the statistical significance of modeling the AMS using the Gumbel distribution.

4.2.2. Developing the IDF Curves

The IDF curves of eight major cities in the UAE were developed using the methodology described in Section 2. The IDF curves developed using 41 years of CHIRPS data for different storm event durations with different return periods are shown in Figure 9. The southwestern part of the country had the lowest IDF precipitation intensities, and the highest were observed in the northern region. Al Ain, the only inland city analyzed, was found to have the lowest IDF rainfall intensity. Ras Al Khaimah exhibits the highest rainfall intensity for all storm event durations. This could be due to the Al Hajar mountain chain causing orographic rainfall with winds coming from the Gulf of Oman. Sherif and Chowdhury [47] found a similar pattern of IDF curve distribution across the country after developing IDF curves using rain gauges. The coastal cities also experienced relatively higher intensities than the inland areas. The main reason for this is that the northwesterly winds bring moisture from the Arabian Gulf and lose the majority of their water content in the coastal area before traveling southward [49].

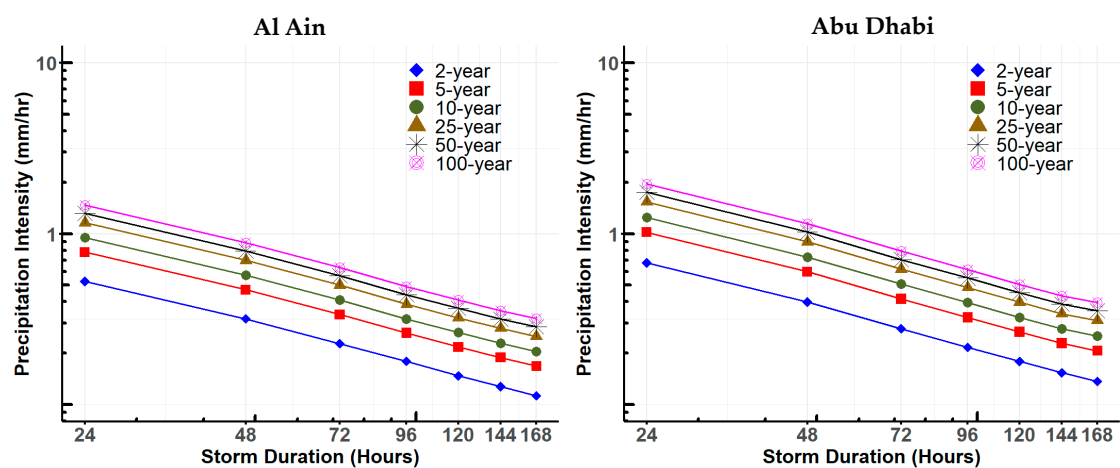


Figure 9. Cont.

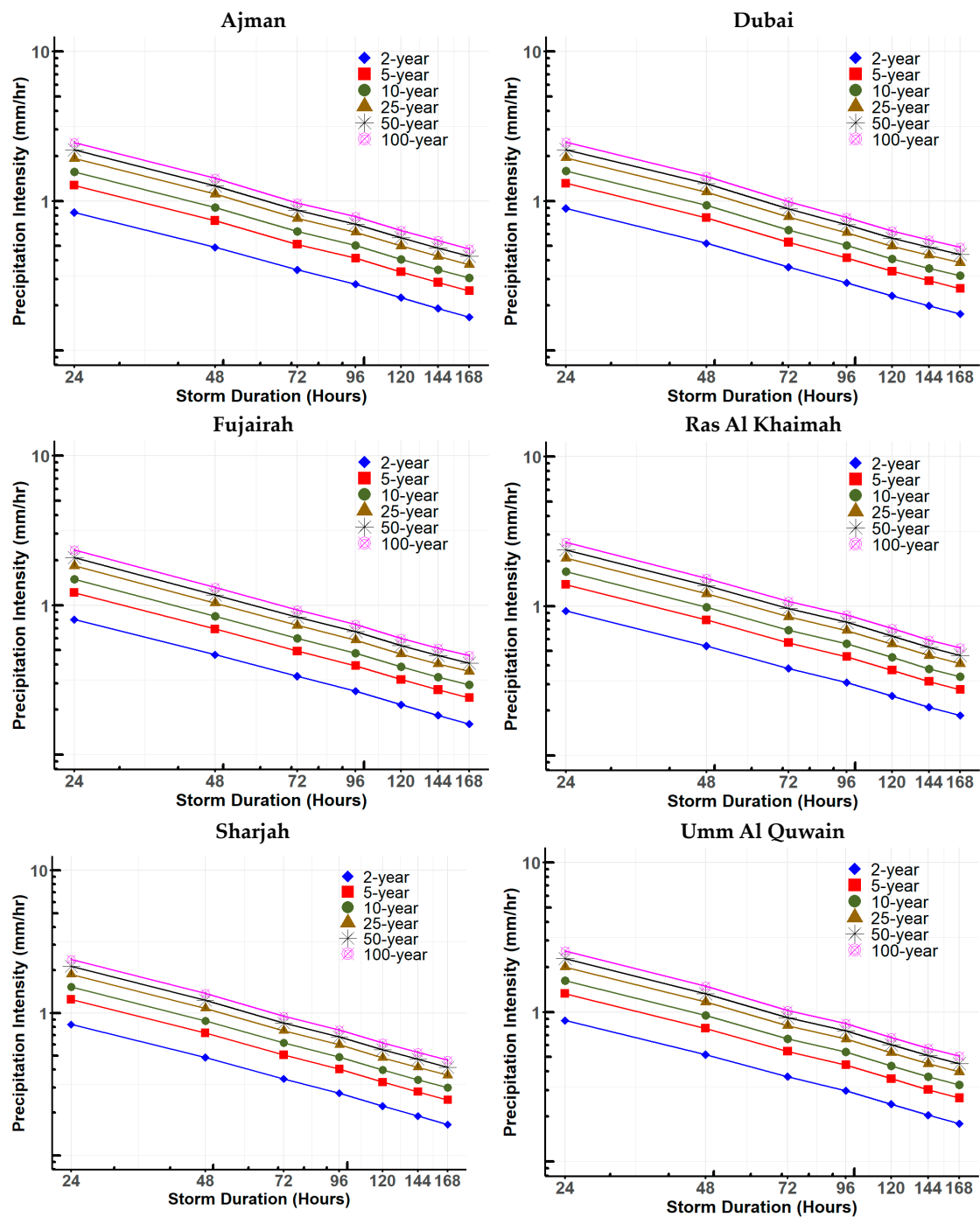


Figure 9. The IDF curves of the eight major cities (Ajman, Dubai, Fujairah, Ras Al Khaimah, Sharjah, and Umm Al Quwain) of the UAE for a storm event duration ranging from 1 days to 7 days for different return period frequencies (both axes are on a logarithmic scale).

The spatial distribution of IDF values aligns seamlessly with the findings of the nationwide IDF analysis. Figure 10 illustrates the spatial distribution of IDF curves for the 1-day storm event across various return periods (10, 25, 50, and 100 years). The spatial pattern reveals that the northeastern region of the UAE, encompassing the Al Hajar Mountain range, consistently exhibits the highest rainfall intensity for all storm event durations. The coastal areas along the Arabian Gulf also demonstrate relatively higher rainfall intensities. Conversely, as anticipated, the southern inland regions consistently exhibit the lowest rainfall intensities across all storm event durations. Similar spatial distributions are observed for durations ranging from 2 to 6 days.

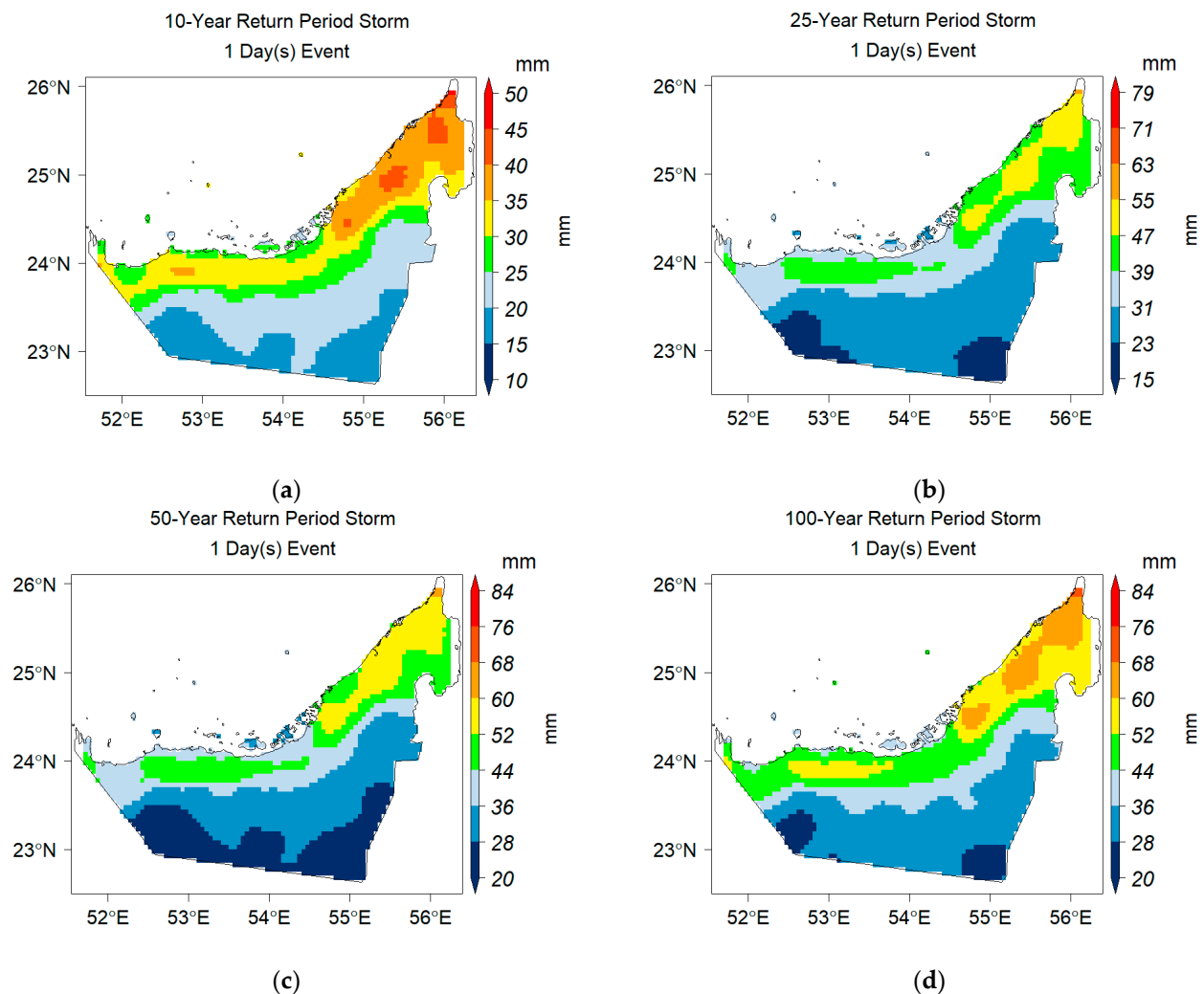


Figure 10. The spatial distribution of the developed IDF curves over the UAE for the (a) 10-year, (b) 25-year, (c) 50-year, and (d) 100-year return periods of the 1-day duration storm event.

5. Conclusions

The recent occurrence of flooding events in the Middle East has brought significant attention to the issue of the assessment of urban flooding, particularly in the United Arab Emirates (UAE). These events have highlighted the vulnerability of coastal regions of the UAE to the impacts of extreme weather events, necessitating a comprehensive evaluation of the risks associated with storms that cause coastal flooding. The exponential growth of urban areas in the UAE has resulted in substantial changes to the landscape and land use patterns. These transformations have led to modifications in surface characteristics, such as increased impervious surfaces, altered drainage patterns, and modifications to natural waterways. These changes, combined with recent climatic changes, necessitate a substantial reform in the approach and frequency of developing and updating IDF curves.

This study introduces a new methodology for developing and updating intensity–duration–frequency (IDF) curves, leveraging a satellite-based precipitation product. Specifically, the CHIRPS dataset was chosen for its extensive historical records, spanning back to 1981. The proposed procedure entails addressing the bias correction of CHIRPS as the initial step, followed by fitting the AMS to a theoretical extreme distribution statistical model. A notable advantage of this methodology is its compatibility with regular updates of IDF curves using more recent datasets. This holds significant importance, particularly in light of incorporating the impacts of rainfall enhancement efforts. A crucial step in the study involved the application of a bias correction factor to the CHIRPS data, yielding

notable improvements in capturing extreme events throughout the country. The correlation between the original data was enhanced from 0.48 to 0.84, showcasing the efficacy of the correction process. Additionally, when comparing the corrected data to validated observations, a correlation of 0.63 was achieved, further validating the accuracy of the methodology. To determine the most suitable theoretical distribution for the UAE, various statistical models were evaluated using criteria such as the Akaike information criterion (AIC) and the Bayesian information criterion (BIC). Among the models considered, the Gumbel distribution emerged as the most appropriate for the majority of the country and across all storm event durations. This selection was driven by the Gumbel distribution consistently exhibiting the lowest AIC and BIC values, indicating a superior fit to the observed data. The results demonstrated that the fit of the Gumbel distribution was deemed suitable for all storm events across over 96% of the country at the 5% significance level. This finding supports the reliability and applicability of the Gumbel distribution in representing the extreme rainfall characteristics in the UAE.

The similarity in shape between the CHIRPS-derived IDF curves and those obtained from rain gauges underscores the reliability of CHIRPS as a data source. The northeastern region, influenced by the Al Hajar mountain chain, experiences the highest IDF intensities due to orographic rainfall. Conversely, the southern inland regions, characterized by aridity, exhibit the lowest IDF intensities. These findings contribute to a comprehensive understanding of rainfall patterns in the UAE and facilitate more effective planning and management of water resources and infrastructure.

This study highlights the immense potential of the CHIRPS dataset for developing IDF curves, owing to its rich historical data and high spatial resolution. The necessity of performing a bias correction is emphasized, underscoring the importance of adjusting the CHIRPS dataset to enhance its accuracy. The choice of adjustment technique should be tailored to the intended purpose of the dataset's application, ensuring its suitability and reliability. By employing these considerations, this study establishes a robust foundation for utilizing the CHIRPS dataset in IDF curve development. Furthermore, it is worth considering the enhancement of the CHIRPS product through the application of machine learning techniques and its integration with other remote sensing rainfall products, such as the GPM-IMERG.

The selection of the most appropriate adjustment technique for the CHIRPS dataset should be guided by the specific application in which the data will be used. The adjustment process should carefully consider the unique characteristics and requirements of the case at hand's intended use. This tailored approach ensures that the CHIRPS dataset is appropriately adjusted to meet the demands of IDF curve development, facilitating precise and reliable estimates of extreme rainfall events. Given the dynamic nature of the UAE's urban landscape, climatic variability and changes, and the ongoing efforts in rainfall enhancement, it is crucial to increase the frequency of IDF curve updates. The regular monitoring of rainfall data, analyses of historical and real-time rainfall patterns, and the incorporation of climate change projections are essential components of an effective and adaptive IDF curve development process.

By implementing a comprehensive overhaul of IDF curve development and update procedures, the UAE can effectively align its flood risk management strategies with the evolving realities of climate change. Accurate and up-to-date IDF curves are indispensable for informed infrastructure design, land use planning, and emergency preparedness. Embracing this reform will empower the UAE to enhance its resilience to shifting precipitation patterns and safeguard its communities and critical assets from the escalating impacts of extreme weather events.

Author Contributions: T.S.A. and K.A.H. guided this research and contributed significantly to preparing the manuscript for publication; T.S.A., K.A.H., P.P., D.T.G., H.O.S. and W.A. developed the research methodology; T.S.A., K.A.H., P.P. and D.T.G. downloaded and processed the remote sensing products; D.T.G. developed the scripts used in the analysis; T.S.A., K.A.H., H.O.S., W.A. and D.T.G. prepared the first draft; T.S.A. and K.A.H., D.T.G., P.P. and H.O.S. performed the final

overall proofreading of the manuscript. All authors have read and agreed to the published version of the manuscript.

Funding: This research was funded through the UAEU Research and Sponsored Projects Office (Grant: G00003477).

Data Availability Statement: The study utilized publicly available datasets, with CHIRPS data accessible at [<https://www.chc.ucsb.edu/data/chirps>]. The article contains additional data that have been used and analyzed.

Acknowledgments: We would like to thank the United Arab Emirates University—Research Affairs for their great support. Gratitude is also extended to Rowan Hussein for editing the manuscript.

Conflicts of Interest: Author Dawit T. Ghebreyesus is employed by the company Bridgefarmer & Associates, Inc. The remaining authors declare that the research was conducted in the absence of any commercial or financial relationships that could be construed as a potential conflict of interest.

References

1. Choubey, S.; Rina Kumari, R.; Chander, S.; Kumar, P. Analysis of Various Gauge Adjusted Merged Satellite Rainfall Products: A study for Major River Basins of Western India. In Proceedings of the EGU General Assembly 2023, Vienna, Austria, 24–28 April 2023; p. EGU23-13962. [[CrossRef](#)]
2. Raj, P.; Padiyath, N.; Semioshkina, N.; Addad, Y.; Foulon, F.; Francis, D.; Voigt, G. Conceptualization of arid region radioecology strategies for agricultural ecosystems of the United Arab Emirates (UAE). *Sci. Total. Environ.* **2022**, *832*, 154965. [[CrossRef](#)] [[PubMed](#)]
3. Chowdhury, R.; Mohamed, M.M.; Murad, A. Variability of Extreme Hydro-Climate Parameters in the North-Eastern Region of United Arab Emirates. *Procedia Eng.* **2016**, *154*, 639–644. [[CrossRef](#)]
4. Sadeghi, M.; Asanjan, A.A.; Faridzad, M.; Nguyen, P.; Hsu, K.; Sorooshian, S.; Braithwaite, D. PERSIANN-CNN: Precipitation Estimation from Remotely Sensed Information Using Artificial Neural Networks–Convolutional Neural Networks. *J. Hydrometeorol.* **2019**, *20*, 2273–2289. [[CrossRef](#)]
5. Ayugi, B.; Tan, G.; Ullah, W.; Boiyi, R.; Ongoma, V. Inter-comparison of remotely sensed precipitation datasets over Kenya during 1998–2016. *Atmos. Res.* **2019**, *225*, 96–109. [[CrossRef](#)]
6. Anderson, R.G.; Lo, M.H.; Famiglietti, J.S. Assessing surface water consumption using remotely-sensed groundwater, evapotranspiration, and precipitation. *Geophys. Res. Lett.* **2012**, *39*, 1–6. [[CrossRef](#)]
7. Luo, X.; Wu, W.; He, D.; Li, Y.; Ji, X. Hydrological Simulation Using TRMM and CHIRPS Precipitation Estimates in the Lower Lancang-Mekong River Basin. *Chin. Geogr. Sci.* **2019**, *29*, 13–25. [[CrossRef](#)]
8. Duan, Z.; Liu, J.; Tuo, Y.; Chiogna, G.; Disse, M. Evaluation of eight high spatial resolution gridded precipitation products in Adige Basin (Italy) at multiple temporal and spatial scales. *Sci. Total. Environ.* **2016**, *573*, 1536–1553. [[CrossRef](#)]
9. Tang, G.; Clark, M.P.; Papalexiou, S.M.; Ma, Z.; Hong, Y. Have satellite precipitation products improved over last two decades? A comprehensive comparison of GPM IMERG with nine satellite and reanalysis datasets. *Remote Sens. Environ.* **2020**, *240*, 111697. [[CrossRef](#)]
10. Sorooshian, S.; AghaKouchak, A.; Arkin, P.; Eylander, J.; Foufoula-Georgiou, E.; Harmon, R.; Hendrickx, J.M.H.; Imam, B.; Kuligowski, R.; Skahill, B.; et al. Advanced Concepts on Remote Sensing of Precipitation at Multiple Scales. *Bull. Am. Meteorol. Soc.* **2011**, *92*, 1353–1357. [[CrossRef](#)]
11. Alsumaiti, T.S.; Hussein, K.; Ghebreyesus, D.T.; Sharif, H.O. Performance of the CMORPH and GPM IMERG Products over the United Arab Emirates. *Remote Sens.* **2020**, *12*, 1426. [[CrossRef](#)]
12. Li, Z.; Yang, D.; Hong, Y. Multi-scale evaluation of high-resolution multi-sensor blended global precipitation products over the Yangtze River. *J. Hydrol.* **2013**, *500*, 157–169. [[CrossRef](#)]
13. Ghebreyesus, D.; Sharif, H.O. Spatio-Temporal Analysis of Precipitation Frequency in Texas Using High-Resolution Radar Products. *Water* **2020**, *12*, 1378. [[CrossRef](#)]
14. Siuki, S.K.; Saghaian, B.; Moazami, S. Comprehensive evaluation of 3-hourly TRMM and half-hourly GPM-IMERG satellite precipitation products. *Int. J. Remote Sens.* **2017**, *38*, 558–571. [[CrossRef](#)]
15. Han, H.; Abitew, A.T.; Seongyu, P.; Grewn, C.H.M.; Jeong, J. Spatiotemporal Evaluation of Satellite-Based Precipitation Products in the Colorado River Basin. *J. Hydrometeorol.* **2023**, *24*, 1739–1754. [[CrossRef](#)]
16. Furl, C.; Ghebreyesus, D.; Sharif, H.O. Assessment of the Performance of Satellite-Based Precipitation Products for Flood Events across Diverse Spatial Scales Using GSSHA Modeling System. *Geosciences* **2018**, *8*, 191. [[CrossRef](#)]
17. Yang, Y.; Luo, Y. Evaluating the performance of remote sensing precipitation products CMORPH, PERSIANN, and TMPA, in the arid region of northwest China. *Theor. Appl. Clim.* **2014**, *118*, 429–445. [[CrossRef](#)]
18. Rivera, J.A.; Marianetti, G.; Hinrichs, S. Validation of CHIRPS precipitation dataset along the Central Andes of Argentina. *Atmos. Res.* **2018**, *213*, 437–449. [[CrossRef](#)]
19. Aksu, H.; Akgül, M.A. Performance evaluation of CHIRPS satellite precipitation estimates over Turkey. *Theor. Appl. Clim.* **2020**, *142*, 71–84. [[CrossRef](#)]

20. Hsu, J.; Huang, W.-R.; Liu, P.-Y.; Li, X. Validation of CHIRPS Precipitation Estimates over Taiwan at Multiple Timescales. *Remote Sens.* **2021**, *13*, 254. [\[CrossRef\]](#)
21. Prakash, S. Performance assessment of CHIRPS, MSWEP, SM2RAIN-CCI, and TMPA precipitation products across India. *J. Hydrol.* **2019**, *571*, 50–59. [\[CrossRef\]](#)
22. Ghebreyesus, D.T.; Sharif, H.O. Development and Assessment of High-Resolution Radar-Based Precipitation Intensity-Duration-Curve (IDF) Curves for the State of Texas. *Remote Sens.* **2021**, *13*, 2890. [\[CrossRef\]](#)
23. Noor, M.; Ismail, T.; Shahid, S.; Asaduzzaman, M.; Dewan, A. Evaluating intensity-duration-frequency (IDF) curves of satellite-based precipitation datasets in Peninsular Malaysia. *Atmos. Res.* **2021**, *248*, 105203. [\[CrossRef\]](#)
24. Monier, E.; Gao, X. Climate change impacts on extreme events in the United States: An uncertainty analysis. *Clim. Change* **2015**, *131*, 67–81. [\[CrossRef\]](#)
25. Rodríguez, R.; Navarro, X.; Casas, M.C.; Ribalaygua, J.; Russo, B.; Pouget, L.; Redaño, A. Influence of climate change on IDF curves for the metropolitan area of Barcelona (Spain). *Int. J. Clim.* **2014**, *34*, 643–654. [\[CrossRef\]](#)
26. Shrestha, A.; Babel, M.S.; Weesakul, S.; Vojinovic, Z. Developing Intensity–Duration–Frequency (IDF) Curves under Climate Change Uncertainty: The Case of Bangkok, Thailand. *Water* **2017**, *9*, 145. [\[CrossRef\]](#)
27. Kidd, C.; Becker, A.; Huffman, G.J.; Muller, C.L.; Joe, P.; Skofronick-Jackson, G.; Kirschbaum, D.B. So, how much of the Earth’s surface is covered by rain gauges? *Bull. Am. Meteorol. Soc.* **2017**, *98*, 69–78. [\[CrossRef\]](#)
28. Ombadi, M.; Nguyen, P.; Sorooshian, S.; Hsu, K. Developing intensity-duration-frequency (IDF) curves from satellite-based precipitation: Methodology and evaluation. *Water Resour. Res.* **2018**, *54*, 7752–7766. [\[CrossRef\]](#)
29. Perica, S.; Pavlovic, S.; Laurent, M.S.; Trypaluk, C.; Unruh, D.; Wilhite, O. Precipitation-Frequency Atlas of the United States, Texas. In *NOAA Atlas 14*; NOAA, National Weather Service: Silver Spring, MD, USA, 2018.
30. Marra, F.; Morin, E.; Peleg, N.; Mei, Y.; Anagnostou, E.N. Intensity–duration–frequency curves from remote sensing rainfall estimates: Comparing satellite and weather radar over the eastern Mediterranean. *Hydrol. Earth Syst. Sci.* **2017**, *21*, 2389–2404. [\[CrossRef\]](#)
31. Sun, Y.; Wendi, D.; Kim, D.E.; Liong, S.-Y. Deriving intensity–duration–frequency (IDF) curves using downscaled in situ rainfall assimilated with remote sensing data. *Geosci. Lett.* **2019**, *6*, 17. [\[CrossRef\]](#)
32. Böer, B. An introduction to the climate of the United Arab Emirates. *J. Arid Environ.* **1997**, *35*, 3–16. [\[CrossRef\]](#)
33. Abrams, M. The Advanced Spaceborne Thermal Emission and Reflection Radiometer (ASTER): Data products for the high spatial resolution imager on NASA’s Terra platform. *Int. J. Remote Sens.* **2000**, *21*, 847–859. [\[CrossRef\]](#)
34. Funk, C.C.; Peterson, P.J.; Landsfeld, M.F.; Pedreros, D.H.; Verdin, J.P.; Rowland, J.D.; Romero, B.E.; Husak, G.J.; Michaelsen, J.C.; Verdin, A.P. A quasi-global precipitation time series for drought monitoring. *US Geol. Surv. Data Ser.* **2014**, *832*, 1–12. [\[CrossRef\]](#)
35. Funk, C.; Peterson, P.; Landsfeld, M.; Pedreros, D.; Verdin, J.; Shukla, S.; Husak, G.; Rowland, J.; Harrison, L.; Hoell, A.; et al. The climate hazards infrared precipitation with stations—A new environmental record for monitoring extremes. *Sci. Data* **2015**, *2*, 150066. [\[CrossRef\]](#) [\[PubMed\]](#)
36. Funk, C.; Verdin, A.; Michaelsen, J.; Peterson, P.; Pedreros, D.; Husak, G. A global satellite-assisted precipitation climatology. *Earth Syst. Sci. Data* **2015**, *7*, 275–287. [\[CrossRef\]](#)
37. Katiraie-Boroujerdy, P.-S.; Ashouri, H.; Hsu, K.-L.; Sorooshian, S. Trends of precipitation extreme indices over a subtropical semi-arid area using PERSIANN-CDR. *Theor. Appl. Clim.* **2017**, *130*, 249–260. [\[CrossRef\]](#)
38. Asong, Z.E.; Razavi, S.; Wheeler, H.S.; Wong, J.S. Evaluation of Integrated Multisatellite Retrievals for GPM (IMERG) over Southern Canada against Ground Precipitation Observations: A Preliminary Assessment. *J. Hydrometeorol.* **2017**, *18*, 1033–1050. [\[CrossRef\]](#)
39. Hussein, K.A.; Alsumaiti, T.S.; Ghebreyesus, D.T.; Sharif, H.O.; Abdalati, W. High-Resolution Spatiotemporal Trend Analysis of Precipitation Using Satellite-Based Products over the United Arab Emirates. *Water* **2021**, *13*, 2376. [\[CrossRef\]](#)
40. Yang, W.; Andréasson, J.; Graham, L.P.; Olsson, J.; Rosberg, J.; Wetterhall, F. Distribution-based scaling to improve usability of regional climate model projections for hydrological climate change impacts studies. *Hydrol. Res.* **2010**, *41*, 211–229. [\[CrossRef\]](#)
41. Omranian, E.; Sharif, H.O. Evaluation of the Global Precipitation Measurement (GPM) Satellite Rainfall Products over the Lower Colorado River Basin, Texas. *JAWRA J. Am. Water Resour. Assoc.* **2018**, *54*, 882–898. [\[CrossRef\]](#)
42. Martins, E.S.; Stedinger, J.R. Generalized maximum-likelihood generalized extreme-value quantile estimators for hydrologic data. *Water Resour. Res.* **2000**, *36*, 737–744. [\[CrossRef\]](#)
43. Martins, E.S.; Stedinger, J.R. Generalized Maximum Likelihood Pareto-Poisson estimators for partial duration series. *Water Resour. Res.* **2001**, *37*, 2551–2557. [\[CrossRef\]](#)
44. Massey, F.J., Jr. The Kolmogorov-Smirnov test for goodness of fit. *J. Am. Stat. Assoc.* **1951**, *46*, 68–78. [\[CrossRef\]](#)
45. Bai, L.; Shi, C.; Li, L.; Yang, Y.; Wu, J. Accuracy of CHIRPS Satellite-Rainfall Products over Mainland China. *Remote Sens.* **2018**, *10*, 362. [\[CrossRef\]](#)
46. Sakib, S.; Ghebreyesus, D.; Sharif, H.O. Performance Evaluation of IMERG GPM Products during Tropical Storm Imelda. *Atmosphere* **2021**, *12*, 687. [\[CrossRef\]](#)
47. Sherif, M.; Chowdhury, R.; Shetty, A. Rainfall and Intensity-Duration-Frequency (IDF) Curves in the United Arab Emirates. In *Proceedings of the World Environmental and Water Resources Congress 2014*, Portland, OR, USA, 1–5 June 2014.

-
48. Almheiri, K.B.; Rustum, R.; Wright, G.; Adeloye, A.J. Study of Impact of Cloud-Seeding on Intensity-Duration-Frequency (IDF) Curves of Sharjah City, the United Arab Emirates. *Water* **2021**, *13*, 3363. [[CrossRef](#)]
 49. Fonseca, R.; Francis, D.; Nelli, N.; Cherif, C. Regional atmospheric circulation patterns driving consecutive fog events in the United Arab Emirates. *Atmos. Res.* **2023**, *282*, 106506. [[CrossRef](#)]

Disclaimer/Publisher’s Note: The statements, opinions and data contained in all publications are solely those of the individual author(s) and contributor(s) and not of MDPI and/or the editor(s). MDPI and/or the editor(s) disclaim responsibility for any injury to people or property resulting from any ideas, methods, instructions or products referred to in the content.